Int J Earth Sciences (Geol Rundsch) (2001) 90:519–533
DOI 10.1007/s005310000183

ORIGINAL PAPER

K. Benedek · Z.R. Nagy · I. Dunkl · C. Szabó
S. Józsa

Petrographical, geochemical and geochronological constraints on igneous clasts and sediments hosted in the Oligo-Miocene Bakony Molasse, Hungary: evidence for a Paleo-Drava River system

Received: 20 April 2000 / Accepted: 15 November 2000 / Published online: 17 March 2001

Abstract The provenance of igneous clasts and arenitic sediment enclosed within the Bakony Molasse was studied using geochemical and geochronological methods. The majority of igneous clasts were eroded from the Oligocene Periadriatic magmatic belt. A part of the andesite material has Eocene formation age. Rhyolitic pebbles originated from Permian sequences of the Greywacke zone or the Gurktal Alps. Apatite fission track (FT) ages from the sandstone matrix (age clusters at ~75 and ~30 Ma) are typical for the Austroalpine nappe pile and for the cooling ages of Periadriatic magmatic belt. Variscan detrital zircon FT ages indicate source areas that had not suffered Alpine metamorphism, such as the Bakony Mountains, Drauzug and the Southern Alps. Another group of detrital zircon grains of Late Triassic–Jurassic FT age (mean: ~183 Ma) marks source zones with Mesozoic thermal overprint such as the Gurktal Alps and some Austroalpine regions. Zircon grains with Oligocene FT age (mean: ~34.7 Ma) were derived from the Periadriatic intrusives and their contact zones. On the basis of the new data, we propose that the ancestor of the recent Drava River had already existed in Oligo-Miocene time and distributed eroded material of the southern Eastern Alps to the east.

Keywords Alpine Molasse · Fission track dating · K/Ar dating · Geochemistry · Provenance analysis · Pannonian Basin · Oligocene–Miocene

K. Benedek (✉) · C. Szabó · S. Józsa
Eötvös University, Department of Petrology and Geochemistry, Múzeum krt. 4/a, Budapest 1088, Hungary
E-mail: bkalman@ludens.elte.hu
Phone: +36-1-2669833
Fax: +36-1-2664992

Z.R. Nagy
Hungarian Academy of Sciences, Geological Research Group, Eötvös University, Múzeum krt. 4/a, Budapest 1088, Hungary

I. Dunkl
Laboratory for Geochemical Research, Hungarian Academy of Sciences, Budaörsi út 45, Budapest 1112, Hungary

Present addresses:
Z.R. Nagy
University of Missouri-Rolla, Department of Geology and Geophysics, 125 McNutt Hall, MO 65409–0410, USA

I. Dunkl
University of Tübingen, Institute for Geology, Sigwartstrasse 10, 72076 Tübingen, Germany

Introduction

The Alpine collision and subsequent uplift resulted in the formation of numerous alluvial systems during Oligo-Miocene time in the Alpine–Carpathian region. Although the deposits of these systems exhibit diverse sedimentary characteristics, they all share in common the presence of similar Oligocene igneous clasts (e.g. tonalites, andesites, dacites, rhyolites) in their coarse debris (Gelati et al. 1988; Stingl and Krois 1991; Rahn et al. 1995; Mair et al. 1996; Ruffini et al. 1997; Brügel 1998; Brügel et al. 2000).

In the Pannonian Basin, Late Oligocene–Early Miocene coarse sands and conglomerates with the same characteristics are exposed between the cities of Sümeg and Mór in the area of the Bakony Mountains (Fig. 1). The lack of a suitable fossil record makes precise biostratigraphic subdivision impossible. The identification of the source area of the magmatic clasts was previously uncertain due to the lack of suitable constraints (Korpás 1981; Báldi 1986).

In this paper we show new petrographic and geochemical results for representative igneous clasts derived from this alluvial system, known as the Csatka Formation. We present detailed petrographic descriptions and geochemical analyses of the clasts and highlight features that are characteristic of the magmatic source. Fission track (FT) and K/Ar geochronology of

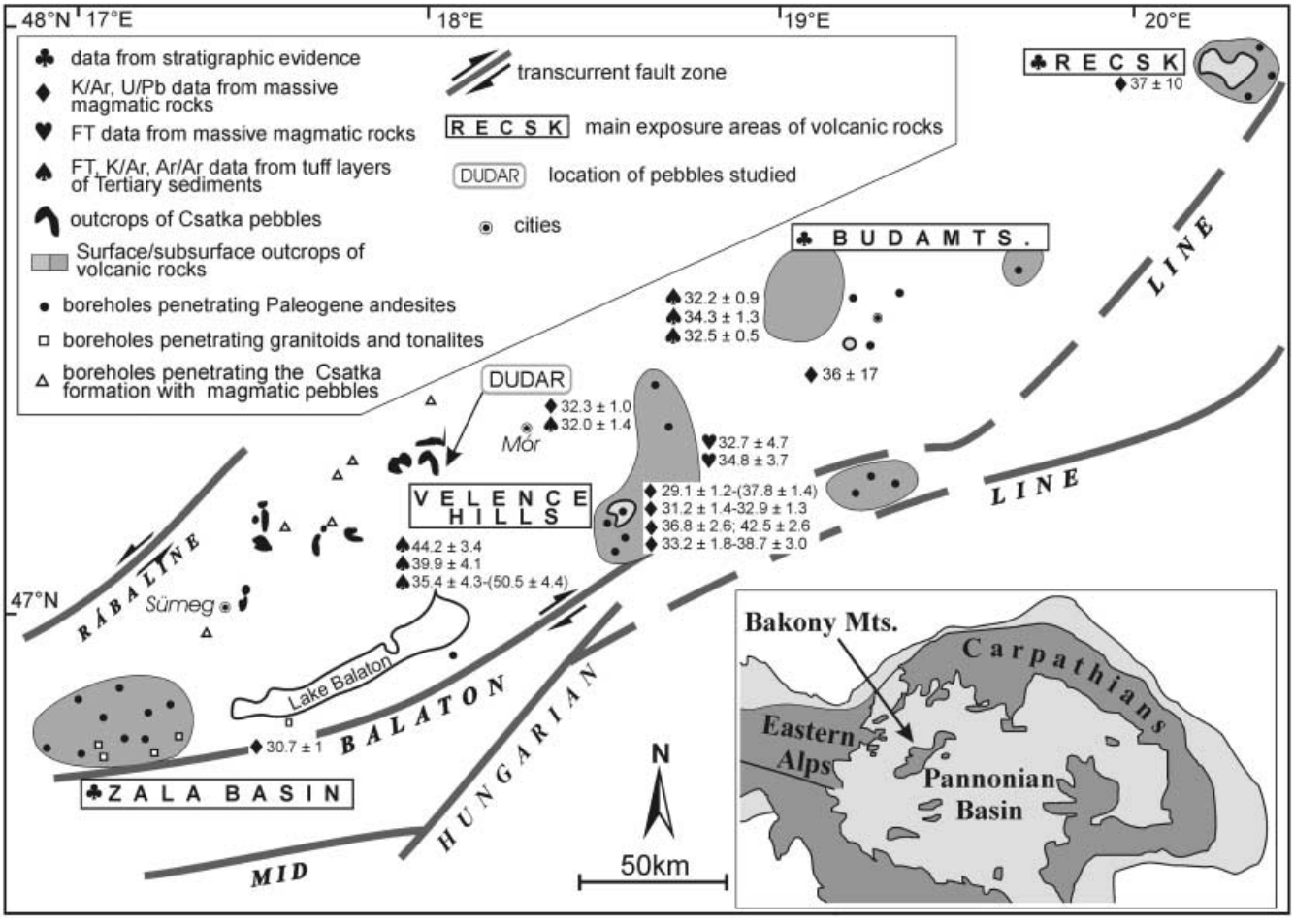

Fig. 1 Locations of Paleogene magmatic rocks in the western Pannonian Basin with a compilation of published geochronological data (Baksa 1975; Balogh 1985; Nagymarosy et al. 1986; Darida-Tichy 1987; Horváth and Tari 1987; Körössy 1988; Dunkl and Nagymarosy 1992). The Velence Hills and surrounding areas towards the Csatka Basin can be ruled out as a source area for igneous clasts (after Korpás 1981)

magmatic clasts and sandstone samples allow us to identify the dominant ages of the eroded materials and suggest likely source areas.

Geological setting

The Bakony Mountains (Fig. 1, hereafter referred to as BM) comprise a complete Variscan–Alpine sequence situated in the Alcapa microplate, Western Hungary. Pre-Late Carboniferous rocks of the unit underwent low-grade, regional pre-Westphalian metamorphism (Árkai and Lelkes-Felvári 1987), and were unaffected by Alpine metamorphism (Lelkes-Felvári et al. 1996). The Variscan sequence includes: (1) Ordovician–Devonian metasiltstones, quartz phyllites, metasandstones and metarhyolites, (2) Early Carboniferous marine molasse, and subsequent (3) Carboniferous granite plutons and Permian dacitic volcanics. Triassic sedimentation was dominantly shallow marine and produced carbonates and claystones accompanied by volcanoclastics (for details see Haas et al. 1995; Harangi et al. 1996). The Jurassic to Early Cretaceous sediments are mainly pelagic and include condensed and incomplete sequences (Vörös and Galácz 1998). Due to Cretaceous orogenic movements there is a stratigraphic gap taking the form of subaerial exposure and deep erosion into the Triassic strata (D'Argenio and Mindszenty 1995).

The Cenozoic sedimentary sequence began in the Eocene (Lutetian). Deepening upward sediments, such as bauxite and coal layers, basal conglomerates, sandstones, nummulitic limestones and marls, accumulated in the basins (Royden and Báldi 1988), occasionally interlayered with tuff horizons (Székyné and Barabás 1953; Balogh 1985; Dunkl 1990). Eocene andesite and calc-alkaline tonalite magmatic rocks intruded into these sediments (Balázs et al. 1981) and have been interpreted on the basis of their chemistry to be subduction-related (Downes et al. 1995). Following this, the western side of the BM was uplifted, partly eroded and an E–W facies polarity initiated (Báldi and Báldi-Beke 1985). In the west, much of the BM was covered by alluvial–brackish sediments, whereas in the east

pelagic marls were deposited. The Oligo-Miocene alluvial sequence, the Csatka Formation (CsF) is characterized by cyclic sedimentation of up to 800-m-thick lacustrine–paludal, flood plain and channel sediments (Korpás 1981). Sedimentary imbrication structures indicate paleotransport from the west to the east.

In the Early and Middle Miocene, the BM extruded eastward as a probable consequence of thermal softening of the nappe stack and continental convergence between Europe and Apulia (Tari et al. 1993; Frisch et al. 1998), although some authors suggest that this motion might also have begun in the Middle Eocene (Kázmér and Kovács 1985; Müller et al. 1996).

Material and methods

Igneous clasts used for petrographic and geochemical analysis were collected from the Dudar coal mine (47°18.5′N; 17°53.6′E; Fig. 1). In spite of intensive weathering, fresh pebbles and mineral separates were readily separated. Microprobe analyses were carried out by using an Amray 1830 I instrument equipped with EDAX 9800 EDS, at an accelerating potential of 15 kV at Eötvös University (Budapest) (Tables 1, 2, 3). Representative bulk samples (Table 4) were analysed for major and trace elements by XRF at Florence University (sample Baz-2, And-97/1, And-94, Du-122, Du-68), Italy (following the method of Franzini et al. 1975) and at XRAL Laboratories (sample G-7, A-12, A-20, QP-2), Ontario (Canada) (details in Norrish and Hutton 1969; Chappell 1991). K/Ar age determinations were carried out on minerals and whole rocks at the Institute of Nuclear Research of the Hungarian Academy of Sciences (ATOMKI) (Table 5). Fission track dating using the external detector technique and zeta calibration was performed in the laboratory of the University of Tübingen (Table 6). The sample processing and system calibration are described in Dunkl and Demény (1997) and Sachsenhofer et al. (1998). Zircon morphology was determined in Entellan (MERCK) immersion using a Zeiss Axiphot microscope, using transmitted light with 200 times magnification. A minimum of 100 crystals were considered.

Petrography

Igneous rocks represent the most distinct spatial and temporal events, and this study therefore focused on magmatic clasts as the best indicator of the probable source regions. Within the clast associations collected from the CsF, five igneous rock types were distinguished, from basaltic to acidic composition.

The grey to black *basaltic andesites* were found to contain phenocrysts of plagioclase, olivine and clinopyroxene in an intergranularly textured groundmass (Fig. 2a). The olivines are completely replaced by

Table 1 Representative microprobe analyses of plagioclases in igneous clasts from the Csatka Formation (*n.d.* not detected)

Mineral	Plagioclase												
Rock	Tonalite						Dacite			Andesite			
Sample	C1	C2	C3	E1	E2	E3	D1	D2	D3	A1	A2	A3	A4
SiO_2	51.67	53.08	51.84	64.89	62.73	63.81	55.45	55.17	55.22	48.80	48.88	53.65	50.62
Al_2O_3	29.46	28.51	29.44	21.58	22.71	22.14	27.15	27.11	27.53	32.46	32.08	28.78	30.63
CaO	12.96	12.20	13.12	2.97	4.88	3.92	10.44	10.33	10.54	15.25	15.59	11.75	13.57
Na_2O	4.73	5.03	4.53	9.31	8.38	8.85	5.86	6.08	6.01	3.34	3.37	5.12	4.17
K_2O	0.39	0.34	0.33	0.57	0.76	0.66	0.30	0.31	0.42	n.d.	n.d.	0.28	0.24
Total	99.21	99.16	99.26	99.32	99.46	99.38	99.21	99.00	99.72	99.85	99.92	99.58	99.23

Table 2 Representative microprobe analyses of amphiboles in igneous clasts from the Csatka Formation (*n.d.* not detected)

Mineral	Amphibole							
Rock	Tonalite		Dacite			Andesite		
Sample	T1	T2	D1	D2	D3	94/1	94/2	94/3
SiO_2	45.33	45.76	45.03	45.35	45.40	44.24	43.43	43.36
TiO_2	1.55	1.43	0.98	0.80	0.93	1.38	1.20	1.27
Al_2O_3	8.90	8.09	9.52	9.62	9.86	11.96	12.07	12.24
FeO	17.88	15.48	17.72	17.88	17.99	14.99	15.17	15.03
MnO	0.25	n.d.	0.66	0.69	0.78	0.49	0.36	0.44
MgO	10.58	11.79	11.18	11.10	11.08	12.14	11.93	12.02
CaO	11.38	11.24	10.24	10.20	10.34	10.97	10.97	10.73
Na_2O	1.83	1.63	1.77	1.89	1.59	2.27	2.48	2.16
K_2O	0.81	0.61	0.46	0.42	0.43	0.57	0.59	0.55
Total	98.51	96.03	97.56	97.95	98.40	99.01	98.20	97.80

Table 3 Representative microprobe analyses of pyroxenes in igneous clasts from the Csatka Formation (*n.d.* not detected)

Mineral	Pyroxene								
Rock	Basalt								
Sample	B1	B2	B3	B4	B5	B6	B7	B8	B9
SiO_2	51.84	51.60	51.26	51.09	51.09	50.34	50.92	50.55	48.93
TiO_2	0.52	0.50	0.63	0.75	0.75	0.80	0.80	0.88	1.20
Cr_2O_3	n.d.	0.56	0.28	0.38	0.47	0.42	0.23	0.48	0.58
Al_2O_3	3.68	3.87	4.16	4.53	4.52	5.57	5.08	5.42	6.82
FeO	5.53	4.86	5.08	5.40	5.40	4.77	6.00	4.88	5.47
MgO	15.33	15.28	14.93	14.74	14.71	14.56	14.48	14.15	13.19
CaO	22.96	23.28	23.52	23.18	23.21	23.45	22.75	23.69	23.37
Total	99.86	99.95	99.86	100.60	100.20	99.91	100.30	100.10	99.56

Table 4 Selected bulk major and trace element compositions of igneous clasts studied from the Csatka Formation (concentrations are given in wt% and ppm respectively, *n.d.* not detected, *b.d.l.* below detection limit)

Sample	Baz-2	And-97/1	A-20	A-12	And-94	Du-122	Du-68	G-7	QP-2
Rock	Basalt	Andesite	Andesite	Andesite	Andesite	Dacite	Tonalite	Tonalite	Rhyolite
SiO_2	53.15	54.83	57.70	59.80	54.01	62.97	73.98	65.10	78.00
TiO_2	1.03	0.76	0.73	0.65	0.84	0.62	0.09	0.57	0.13
Al_2O_3	20.85	18.35	17.00	17.50	16.95	17.82	13.46	16.00	11.10
FeO	2.65	3.96	3.76	3.33	3.76	2.01	1.00	2.12	0.54
Fe_2O_3	4.77	3.68	3.50	3.09	2.86	3.27	0.43	3.45	0.88
MnO	0.06	0.14	0.32	0.05	0.18	0.05	0.03	0.09	0.02
MgO	2.63	2.68	2.98	3.30	2.82	1.64	0.45	1.73	0.19
CaO	5.37	7.01	6.80	5.09	8.11	4.01	2.05	3.78	0.88
Na_2O	2.87	2.39	1.61	1.78	2.71	2.41	2.28	2.50	0.10
K_2O	2.15	1.60	0.62	1.63	1.26	2.31	5.33	2.65	6.83
P_2O_5	0.30	0.30	0.14	0.13	0.23	0.17	0.02	0.16	0.05
LOI	4.17	4.31	3.80	3.65	6.27	2.72	0.87	1.55	1.50
Total	100.00	100.01	98.96	100.00	100.00	100.00	99.99	99.71	100.23
Ni	n.d.	10	9	14	1	b.d.l.	2	15	18
Cr	12	38	17	45	34	13	5	17	n.d.
Co	10	14	11	13	15	8	2	9	4
V	194	126	n.d.	n.d.	150	107	22	n.d.	n.d.
Nb	5	13	7	9	10	12	4	13	12
Zr	147	129	105	117	110	142	86	145	77
Y	20	18	22	22	13	14	31	19	7
Ba	404	317	254	432	356	493	351	554	298
Sr	183	309	276	367	654	217	124	286	44
Rb	53	69	26	71	49	90	114	117	303
Th	b.d.l.	4	7.4	7	7	10	n.d.	17	17
Pb	13	10	63	10	9	16	37	38	15
Zn	71	77	1000	100	70	46	23	100	n.d.
La	30	22	21	20	23	28	21	35	20
Ce	65	49	40	41	56	62	53	66	39
Nd	31	21	18	26	26	27	23	24	14

chlorite and the plagioclase phenocrysts show partial alteration to epidote or carbonate. The homogeneous cores of twinned plagioclase are mantled by narrow reaction zones and oscillatory zoned overgrowths. Clinopyroxene is mostly replaced by carbonates, but there are relicts of former phenocrysts. The groundmass consists of small plagioclase and opaque minerals.

The *andesites* containing plagioclase, biotite, amphibole, augite and quartz were found to be the most common pebble type (Fig. 2b). They have a porphyritic texture with a microcrystalline to glassy matrix. The cores of some plagioclase display normal zoning with a thin reaction zone at the boundary, whereas overgrowth shows oscillatory zoning. Remelted margins can be seen on quartz phenocrysts. Some larger amphiboles have reaction rims containing clinopyroxene, plagioclase and opaque minerals (Fig. 2c). Plagioclase and clinopyroxene are pervasively altered to carbonates or clay minerals, whereas biotite and amphibole are partially chloritized or replaced by opaque minerals. Some andesites contain inclusions of tonalite (Fig. 2d) and mafic rock (Fig. 2e). The mafic inclusions contain elongated amphibole and plagioclase.

The *dacites* have a porphyritic texture with plagioclase, quartz, biotite and amphibole phenocrysts (Fig. 2f). Some dusty plagioclase phenocrysts show

Table 5 K/Ar results for igneous clasts from the Csatka Formation

Occurrence Rock type	Measured fraction	K-content (%)	40Ar rad/g (cm^3 STP/g)	40Ar rad (%)	K/Ar age (Ma)
Dudar QP-2 Rhyolite	Feldspar	5.747	5.3561×10^{-5}	89.5	225±8.5
Dudar VR-1 Red rhyolite	Whole rock	0.77	6.5952×10^{-6}	83.6	208±7.9
Dudar Baz-2 Bas. andesite	Whole rock	1.94	2.6527×10^{-6}	42.4	34.8±1.6
Dudar A-97/1 Andesite	Whole rock	1.648	2.1314×10^{-6}	57.2	33.1±1.4
Dudar A-13 Andesite	Plagioclase	1.774	2.2738×10^{-6}	36.2	32.7±1.6
Dudar Q-7 Tonalite Dudar Q-7	Biotite	4.995	6.1643×10^{-6}	63.9	31.5±1.25
Tonalite	Plagioclase	1.988	2.5394×10^{-6}	45.8	32.6±1.43

Table 6 Apatite and zircon FT results for magmatic and sedimentary samples from the Csatka Formation. *Cryst* Number of dated apatite crystals. Track densities (ρ) are as measured ($\times10^5$ tr/cm^2); number of tracks counted (N) shown in parentheses. Apatite ages calculated using dosimeter glass: CN 5 with ζ_{CN5}=373±7. Zircon ages calculated using dosimeter glass: NBS 962 with ζ_{962}=363.5±6. $P(\chi)$: probability obtaining chi-square value for n degree of freedom (where n=no. crystals–1)

Code	Mineral	Petrography	Cryst.	Spontaneous		Induced		Dosimeter		$P(\chi)$	FT age[a]
				ρs	(Ns)	ρi	(Ni)	ρd	(Nd)	(%)	(Ma±1σ)
Single pebbles											
A-22	Ap.	Andesite pebble	26	1.45	(615)	7.48	(3143)	7.93	(18449)	87	**28.9±1.4**
Z-10	Zi.	Andesite pebble	21	37.0	(1801)	38.2	(1863)	1.50	(5826)	<1	*27.2±1.1*
DUD-3	Zi.	Rhyolite pebble	10	163	(1060)	34.8	(222)	1.74	(2089)	<1	*161±13*
DUD-4	Zi.	Rhyolite pebble	10	188	(611)	41.2	(131)	1.74	(2089)	84	**146±15**
PPD samples											
DUD-6	Ap.	Tonalite pebble population	45	5.30	(829)	13.0	(2038)	4.45	(4448)	52	**33.7±1.6**
DUD-2	Zi.	Andesite pebble population	45	48.4	(2211)	46.3	(2179)	1.74	(2089)	2	*34.3±1.4*
Sandstone samples											
DUD-1	Ap.	Sandstone	45	5.59	(1147)	7.79	(1648)	4.45	(4448)	<1	*67.1±3.0*
DUD-1	Zi.	Sandstone	56	102	(5389)	44.2	(2298)	1.74	(2089)	<1	*119.0±4.4*

[a] Bold, pooled age, italics, mean age

typical mantled structures (see above). The small quartz phenocrysts are partly resorbed, amphiboles are euhedral or subhedral and they are partially replaced by chlorite. Biotite containing plagioclase inclusions exhibits various degrees of alteration into opaque minerals and chlorite.

The *tonalites* were found to have a medium to fine-grained granular texture with euhedral to subhedral phenocrysts (Fig. 2g). Plagioclase dominates (size up to 2 mm) with less abundant biotite and K-feldspar, quartz, amphibole and minor clinopyroxene, epidote and magnetite. Plagioclase is zoned and twinned, and in some cases the core is overgrown by a thick rim. In many samples the feldspars have a thin reaction zone, as in the andesites and dacites (see above). Subhedral and anhedral amphiboles are generally intensively altered to chlorite. Quartz is anhedral and contains grains of the other constituents.

Rhyolite clasts found are small and red in color. Rhyolites consist of partly resorbed anhedral quartz, euhedral plagioclase without dusty zones, and scarce biotite (Fig. 2h). The mafic phenocrysts are intensively altered to chlorite and carbonate.

Mineral chemistry

Plagioclase phenocrysts (Tables 1, 2. 3) were found to have a composition of $An_{37–82}$ in tonalites and $An_{28–50}$ in dacite and andesite. Amphiboles show varying chemical composition in the tonalites and andesites (Tables 1, 2. 3). Magnesio-hornblende occurs in the tonalites and dacites, whereas tschermakitic hornblende or magnesio-hastingsitic hornblende is found in the andesites (Leake et al. 1997). Amphiboles in the andesites were found to contain the lowest SiO_2 (43–44 wt%), FeO (14–15 wt%) and the highest MgO (~12 wt%) and Na_2O (~2 wt%). The composition of clinopyroxene in the basaltic andesite is diopsidic (Table 1, 2. 3) with values ranging from $Wo_{47}En_{43}Fs_{10}$ to

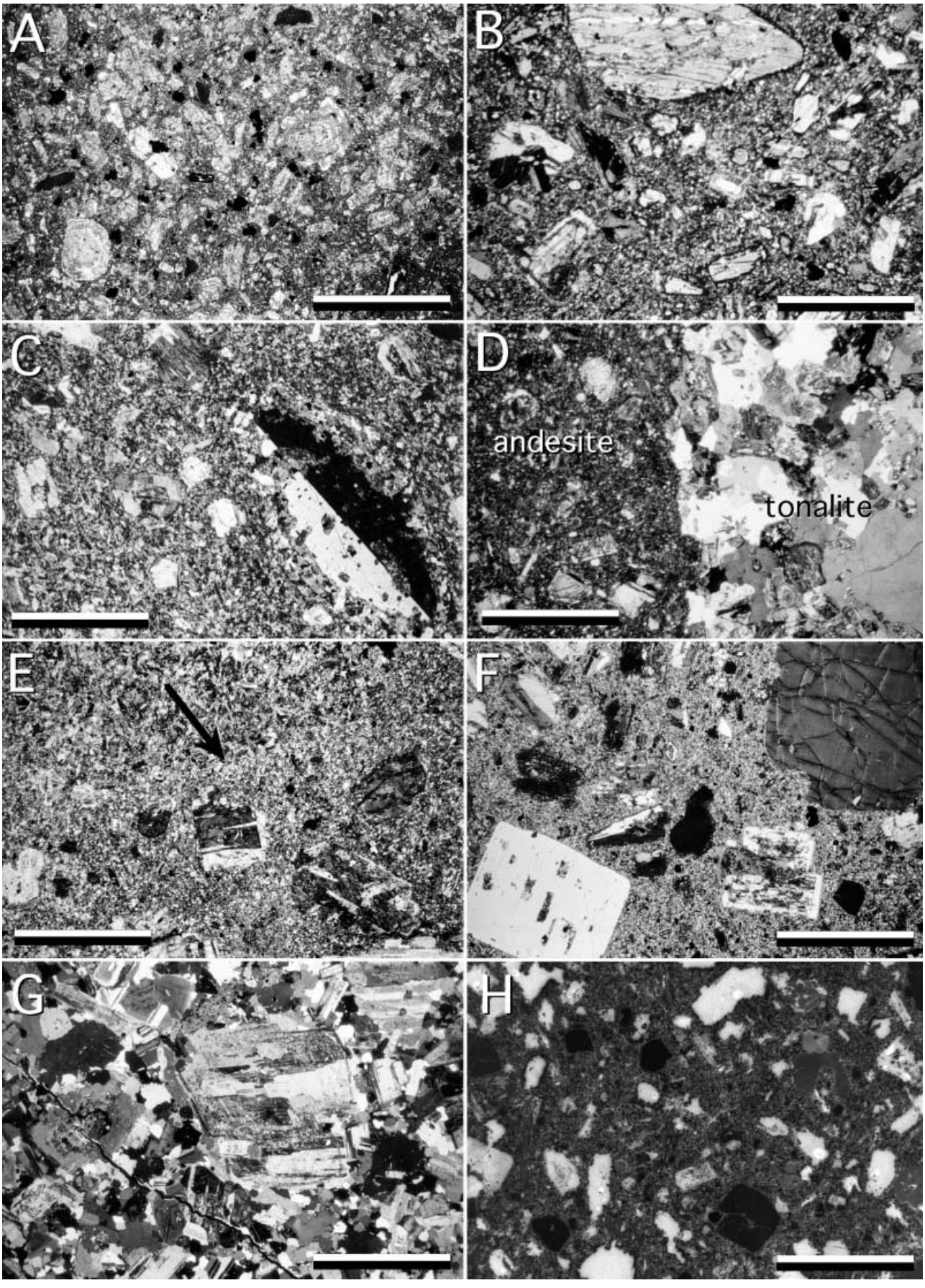
A
B
C
D
andesite
tonalite
E
F
G
H

Fig. 2 Photomicrographs of representative magmatic pebbles found in the Csatka Formation: **A** basaltic andesite, **B** andesite, **C** amphibole phenocryst surrounding by clinopyroxene reaction rim in andesite, **D** tonalite inclusion in andesite, **E** mafic rock inclusion in andesite, **F** dacite, **G** tonalite, **H** rhyolite (for details see the text)

$Wo_{50}En_{41}Fs_9$. The chemical composition of the clinopyroxenes was found to be uniform with SiO_2 between 50 and 51 wt%, MgO between 14 and 15 wt% and CaO between 22 and 23 wt%.

Bulk major and trace element chemistry

The representative samples (Table 4) cover a wide range of compositions from 55 to 74 SiO_2 wt% on the TAS diagram (Fig. 3). Clasts with a low-K, tholeiitic signature were not found in the CsF. The iron–magnesium–total alkali contents of the samples indicate a calc-alkaline character. On the representative Harker variation diagrams (Fig. 4) the relatively immobile elements such as Al_2O_3, MgO and TiO_2 display distinct linear trends. Basaltic andesite and andesite clasts are marked by anomalously high Al_2O_3 (17.7–21.7 wt%) and low MgO (2.7–3.4 wt%).

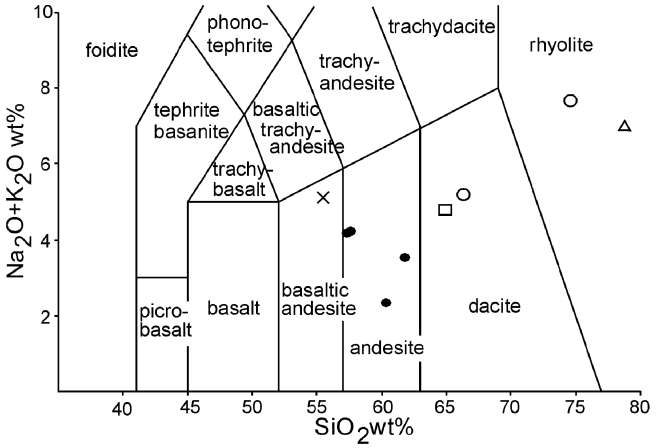

Fig. 3 $K_2O + Na_2O$ vs. SiO_2 diagram of the igneous clasts found in the Csatka Formation. *Cross* basaltic andesite; *filled circle* andesite; *open square* dacite; *open circle* tonalite; *open triangle* rhyolite

The MORB-normalized multielement diagram (Fig. 5) displays relative enrichment in most trace elements but depletion in some compatible elements such as Ni and Cr. A significant negative anomaly in Nb, as seen in the data, is often interpreted as evidence of subduction-related magmatism. Peaks in

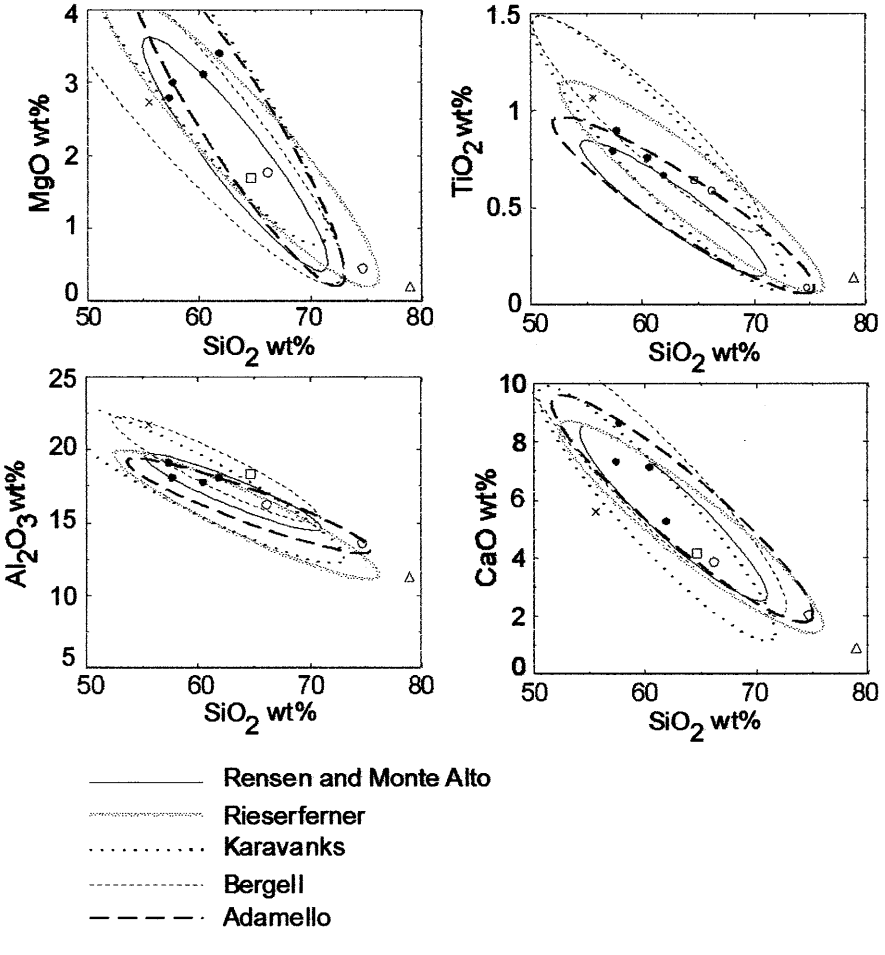

Fig. 4 Representative Harker diagrams of calc-alkaline magmatic rocks found in the Csatka Formation. Legend as in Fig. 3. Data for intrusive rocks from the Periadriatic lineament are also shown for comparison (Faninger 1976; Wenk et al. 1977; Bellieni et al. 1981; Macera et al. 1983; Bellieni et al. 1984)

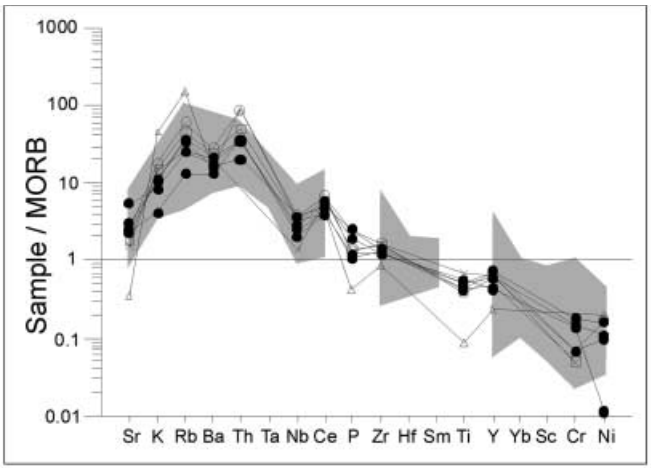

Fig. 5 MORB-normalized (Pearce 1982) trace element diagram for igneous clasts found in the Csatka Formation. The rhyolite clast differs significantly from the other magmatic pebbles. *Shaded area* represents trace element pattern of intrusive rocks from the Periadriatic lineament (Faninger 1976; Bellieni et al. 1981, 1984; Macera et al. 1983). Legend as in Fig. 3

Rb and Th and a trough in Ba are likely to be related to the effects of magmatic processes such as crustal contamination or fractional crystallization or may represent fluids derived from the subducted slab. The rhyolite shows the lowest concentration of Sr, Ti, P and Y and the highest K and Rb content, and has a significantly different trace element chemistry to other igneous pebbles. The Y concentration in the analysed samples is lower than that in MORB.

Geochronology

K/Ar and FT (Tables 5 and 6) measurements were carried out on igneous clasts from Dudar coal mine to constrain the age and source of the volcanic clasts.

The basaltic andesite, andesite and tonalite single clasts gave Oligocene (FT: 33–27 Ma) ages, which overlap with ages of magmatic activity identified along the Periadriatic line (e.g. Blanckenburg and Davies 1995).

The method of pebble population dating (PPD) as discussed in Dunkl et al. (1996) was carried out on two samples by amalgamation of 37 pebbles of tonalite and 169 of andesite to characterize the bulk mass of volcanogenic material. The high number of pebbles reduced the bias of a few individual pebbles which were extremely rich in apatite or zircon. The composite pebble samples were processed and dated in a similar way to sedimentary samples and the individual grain ages were presented in age probability density plots (hereafter referred to as age spectra) according to Hurford et al. (1984). Coal petrological studies show low maturation (VR: Ro<0.4%; Z.A. Horváth, personal communication) and, consequently, no thermal overprint was identified in the samples. Thus, the apatite age spectra represent the FT age distribution of the given lithology exposed in the source area of the sediment in the Late Oligocene.

The tonalite PPD sample passed the chi-square test indicating a homogeneous source (see Table 6), which is rare in the case of composite samples. Thus, the dated grains were derived from a source of homogeneous apatite FT age (Fig. 6a). The pooled apatite FT age of the crystals (33.7 Ma) is within the range of the Periadriatic intrusives (Blanckenburg and Davies 1995).

The andesite PPD sample gave a more complex age spectrum (Fig. 6b) and the sample failed the chi-square test. This distribution indicates that andesite clasts in the CsF are derived from both the Eocene and the Oligocene volcanic cycles. No andesitic material with a Mesozoic FT age was found.

The Triassic K/Ar (225–208 Ma) and Jurassic zircon FT ages (161–146 Ma) of the rhyolite clasts suggest that the drainage area of the CsF contained Mesozoic igneous suites or Paleozoic ones overprinted during Mesozoic thermal events.

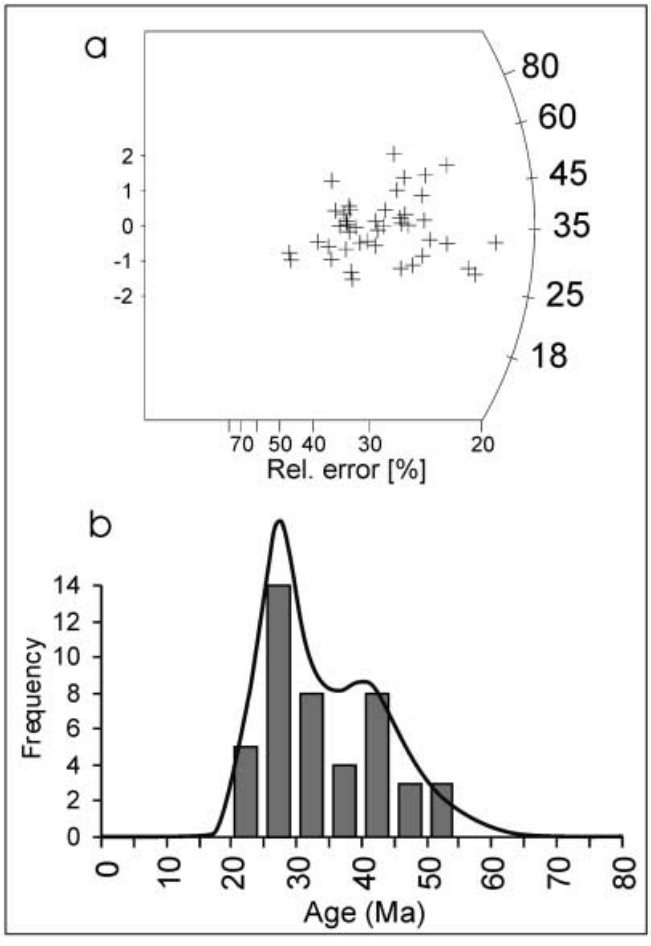

Fig. 6 Age distribution of pebble population (PPD) samples. **a** Apatite ages of the composite sample made from 37 tonalite pebbles; **b** zircon age spectrum of the andesite composite sample made from 169 pebbles

The geochronological data prove that the volcanogenic material was derived from distinct sources.

Discussion

Igneous clasts in the CsF show a wide range of petrologic and geochemical characteristics. However, with the exception of the rhyolite clasts, a close genetic relationship is apparent between the magmatic rocks because: (1) trace element ratios are similar, as seen on the MORB-normalized multielement diagram (Fig. 5), and (2) geochronological data scatter around the peak of the Oligocene Alpine magmatism (~30 Ma). Furthermore, the occurrence of tonalite inclusions in the andesite (Fig. 2d) suggest that both rock types are from the same region.

In contrast, the rhyolite clasts are older and have a very different trace element geochemistry, as seen in the MORB-normalized multielement diagram (Fig. 5).

Character of magmas

Although the basaltic andesite is the least evolved rock type among the clasts in the alluvial succession, it cannot be taken as a primary melt in the magmatic system because plagioclase phenocrysts display a tens of micrometres wide dusty zone, indicating a complex magmatic history (Tsuchiyama 1985) during its evolution. In addition, MgO, Ni and Cr concentrations are very low (Table 4), suggesting that this rock should be highly fractionated and such melts can be produced by olivine–clinopyroxene fractionation from more basaltic melts (e.g. Gill 1981). However, on the basis of experimental studies, olivine does not occur on the liquidii of melts (Myers and Johnston 1996, additional references therein) showing high Al_2O_3 and low MgO content similar to those of our samples. Therefore, it is very difficult to establish the origin of such melts. The magma, which formed the mafic inclusions in the andesite, is a better candidate for the mafic end member, but the size of the inclusions was too small to be analysed for major and trace elements.

Discriminant diagrams for clinopyroxene (Leterrier et al. 1982) from representative basaltic andesite were used (Fig. 7) in order to obtain information about the character of the former melts. The non-alkaline (tholeiitic or calc-alkaline) character of all the clinopyroxenes is apparent. Based on the iron–magnesium–total alkali content, a calc-alkaline character is more likely than a tholeiitic one for the parental magma. The clinopyroxenes plot in the field of orogenic basalts. Furthermore, the La/Th (3–5) and La/Nb (2–6) ratio of andesites (Table 4) also suggest an orogenic magmatic source in the plot of Gill (1981) for calc-alkaline rocks. The data on the multicomponent discrimination diagram of clinopyroxenes (Nisbet and Pearce 1977) plot into the volcanic arc basalt field, suggesting that volcanism took place in a subduction-related environment (Fig. 7).

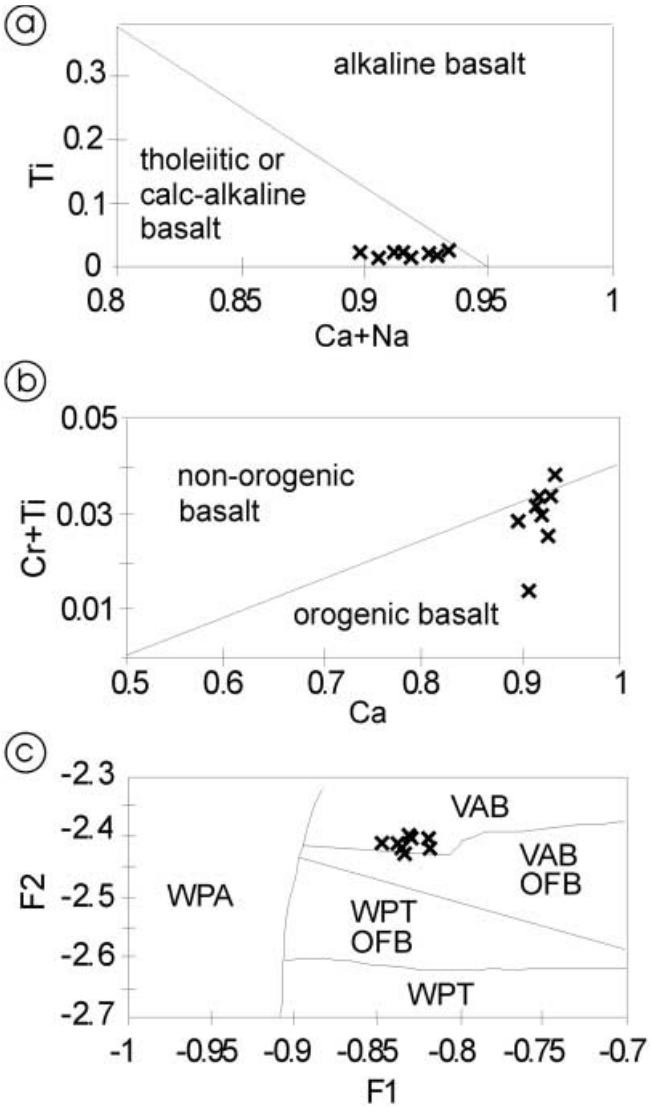

Fig. 7 Discrimination diagrams of clinopyroxenes studied in basaltic andesite clasts from the Csatka Formation. **a** The host magma is tholeiitic or calc-alkaline (Leterrier et al. 1982). **b** Data for clinopyroxenes fall within the orogenic field with the exception of only one sample. **c** Multielement discriminant diagram (Nisbet and Pearce 1977) for pyroxenes showing fields for volcanic arc basalt (*VAB*), ocean-floor basalt (*OFB*), within-plate tholeiitic basalt (*WPT*) and within-plate alkalic basalt (*WPA*). The elements are calculated as cationic values

The calc-alkaline andesite pebbles in the CsF are associated with small mafic, amphibole-rich inclusions (Fig. 2e). The presence of mafic inclusions with a distinctive texture and composition in more evolved calc-alkaline rocks suggests widespread magma mixing (Eichelberger 1978; Bacon 1986). In addition, plagioclase phenocrysts in each host rock type have a narrow dusty zone between the core and rim (Fig. 2a, b, f, g). This is due to the reaction between the plagioclase

core and the hotter, mafic magma (Tsuchiyama 1985). These features are typical of calc-alkaline rocks.

Origin of Pre-Tertiary volcanic clasts

The rhyolite clasts show Late Triassic whole rock K/Ar ages. The zircon FT thermochronometer has a lower closure temperature, and the Jurassic FT ages were therefore formed during thermal resetting (Table 5 and 6). These clasts originated from Permian or Early Paleozoic volcanic bodies which are widespread within the BM, the Southern Alps and the Austroalpine area (Leonardi 1967; Oberhauser 1980). The Jurassic zircon ages exclude derivation from the BM and from the Southern Alps, as their post-Variscan sequences are unmetamorphosed (Lelkes-Felvári et al. 1996). However, a large part of the rhyolitic bodies of the Upper Austroalpine nappe pile underwent low-grade metamorphism during the Mesozoic era (Kralik et al. 1987; Dunkl et al. 1999). These facts imply that the source region of the rhyolitic clasts was in the Eastern Alps, perhaps in the Permian sequence at the base of the Northern Calcareous Alps, in the Greywacke zone or in the Gurktal Alps.

Origin of Paleogene volcanic clasts

The andesite PPD samples revealed two age clusters (see Fig. 6b); the older one is synchronous with the well-documented tuffites of Late Eocene age of the BM (Székyné and Barabás 1953; Dunkl 1990; Dunkl and Nagymarosy 1992). Effusive and dyke rock occurrences of Eocene age are known in the Zala Basin, Velence Hills and at Recsk (Fig. 1; Baksa et al. 1974; Darida-Tichy 1987; Körössy 1988). However, the east-directed transport in the alluvial system eliminates the Velence Hills or Recsk as potential source regions (Korpás 1981). The younger age cluster of the andesite PPD sample (Fig. 6b) is around 30 Ma, which is considered the main period of the Oligocene magmatic activity along the Periadriatic lineament (Blanckenburg and Davies 1995).

Zircon morphological analysis (Pupin 1980) was used for better identification of the source(s) of the magmatic clasts with Paleogene FT ages. The andesite pebble population of the Csatka Formation has a rather diffuse distribution, which is in accord with the composite character of the sample (Fig. 8a). This pattern shows a more complex source than the andesite samples from the Paleogene volcanic edifices of the Pannonian Basin (Fig. 8b). In contrast, the Paleogene igneous rocks situated at the western part of the Pannonian Basin System, along the Drau valley, can be characterized by a broad distribution and they also show similarities to the composite sample of CsF (Fig. 8c). This suggests that the magmatic clasts of Paleogene FT age originate both from the Zala Basin and from the Eastern Alps.

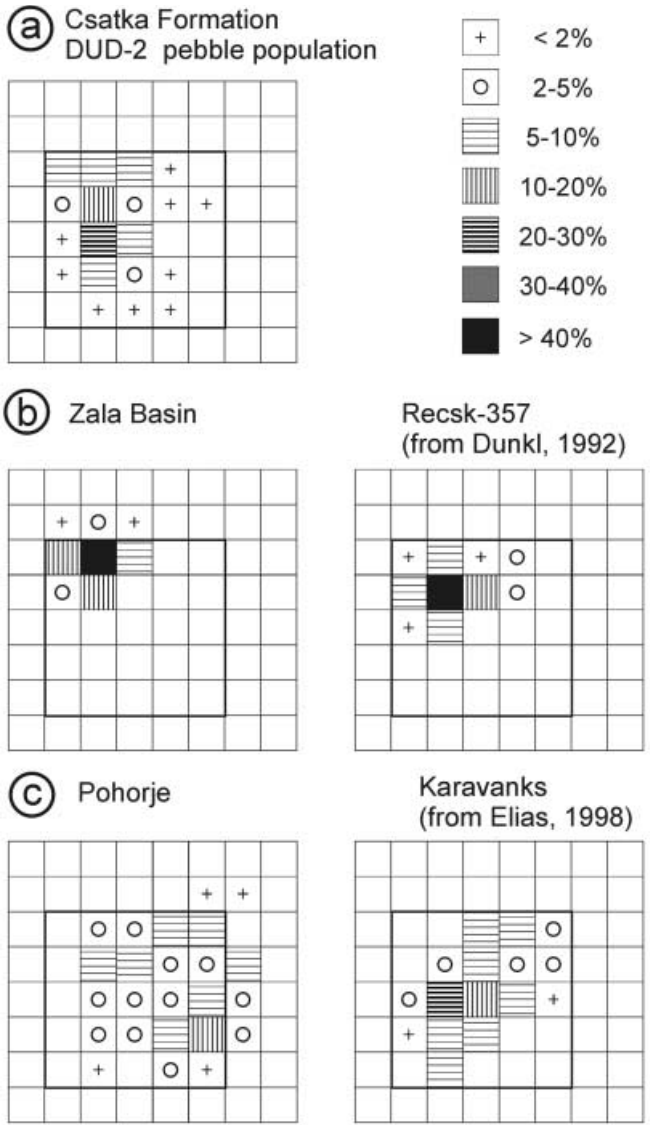

Fig. 8 Morphological classification of zircon crystals according to Pupin (1980). **a** Morphological distribution of the pebble population sample made from andesite clasts of the Csatka Formation. **b** The major Eocene andesite volcanoes of the Pannonian Basin show a tight cluster in the calc-alkaline field. **c** The tonalite bodies exposed along the Drau valley have a broader distribution in zircon morphology, showing similarities to the magmatites of the Csatka Formation

Fission track age of detrital apatite and zircon grains in the sandstone

Detrital apatite crystals in the siliciclastic sandy material from the conglomerate of CsF reflect the entire catchment area of the river system at the time of deposition. During the dating procedure of the sandstone sample, apatite crystals derived from the Paleogene

volcanism (typically big, colourless, euhedral, clear crystals) were not dated. Only the irregular, inclusion-rich apatite grains characteristic of metamorphic rocks, were considered. These grains yielded a bimodal age distribution with the clusters having mean values of approximately 75 and 30 Ma (Fig. 9). The older cluster is typical for the Austroalpine nappe pile (Frank et al. 1987). The apatite grains of the Oligocene age cluster might have been derived from the contact metamorphic aureoles of the Periadriatic tonalite intrusions and/or from exhumed crystalline slabs of Oligocene cooling age situated along the Periadriatic lineament. Resetting and rapid exhumation from the apatite partial annealing zone in the Oligocene within the surroundings of the western Pannonian Basin occurred only along the Periadriatic lineament (Gieger and Hurford 1989; Hejl 1997; Läufer et al. 1997; Sachsehofer et al. 1998).

Zircon FT ages refer to a higher temperature during cooling of metamorphic rocks than apatite ages. The closure temperature, considered to be between 175 and 250 °C (Harrison et al. 1979; Hurford 1986) for zircon, preserves the cooling ages of the last metamorphic overprint. The areal zircon FT age pattern of an orogen is less sensitive to the depth of erosion than the apatite age pattern. Figure 10 shows the zircon age spectrum of a sandstone sample. A Variscan, a Mesozoic and a Paleogene age cluster can be distinguished.

The oldest grains (mean: ~343 Ma) were derived from the basement or from the Permian sequence of the BM, the Drauzug or the Southern Alps. The Late Variscan red sandstone formations are rich in zircon grains and are unmetamorphosed in the structural units listed above, so the original Variscan cooling ages are preserved.

The Mesozoic age cluster (mean: ~183 Ma) could not have been derived from the BM or from the Southern Alps, as no Mesozoic thermal overprint is known from these regions. However, the Late Triassic–Jurassic thermal overprint did reset the zircon FT geochronometer within the western Austroalpine basement (Flisch 1986), the Permo-Scythian sequences of the Northern Calcareous Alps (Elias 1998), the Gurktal Alps and the Austroalpine stripes south of the Tauern Window (Dunkl et al. 1999).

The zircon grains of Paleogene age were mainly derived from the decomposition of igneous rocks. The chi-square age of the youngest population is 34.7± 1.6 Ma calculated according to Brandon (1992). The age of the clear, colourless and fully euhedral grain population falls within the age range of Periadriatic igneous rocks (Fig. 11a). A few rounded zircon grains derived from metasedimentary rocks with an Oligocene cooling age suggest that the deep contact or reset zone of the Periadriatic intrusions were also eroded.

The comparison of the zircon age spectra to the compilation of the zircon FT ages of the Eastern Alps

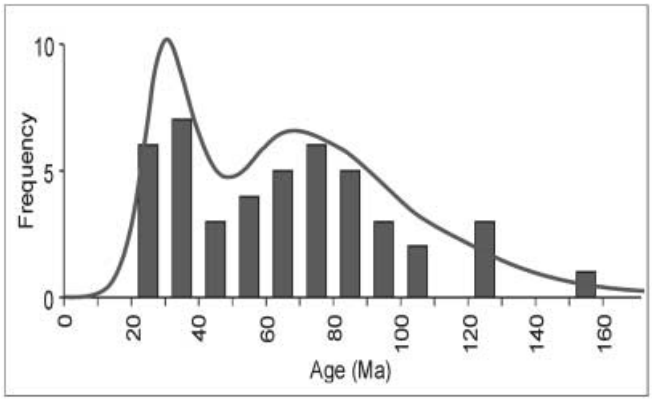

Fig. 9 Fission track age spectrum of the non-volcanogenic apatite grains of a sandstone sample from the Csatka Formation

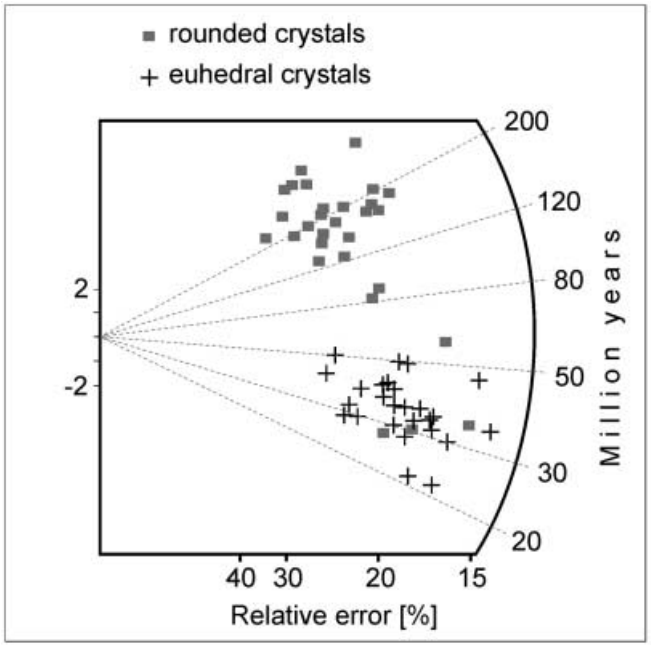

Fig. 10 Radial plot of zircon FT ages of a sandstone sample from the Csatka Formation. The Paleogene age cluster is composed mainly of euhedral crystals derived from Periadriatic intrusive and volcanic rocks

(Fig. 11a, b) shows significant differences. The thermotectonic history of the Eastern Alps consists of two main events: a Late Cretaceous and a Miocene cooling period following the metamorphic climaxes. These cooling events are reflected in the distribution of radiometric ages (Frank et al. 1987). The most characteristic features of the major part of the amphibolite facies rocks within the metamorphic suites of the Austroalpine basement are mica Ar/Ar and Rb/Sr cooling ages of 110 to 70 Ma and slightly younger zircon FT cooling ages (mainly between 80 and 60 Ma, see Fig. 11b). The nearly complete lack of such grains in the CsF can be explained in three different ways: (1) the catchment area did not reach the central crystal-

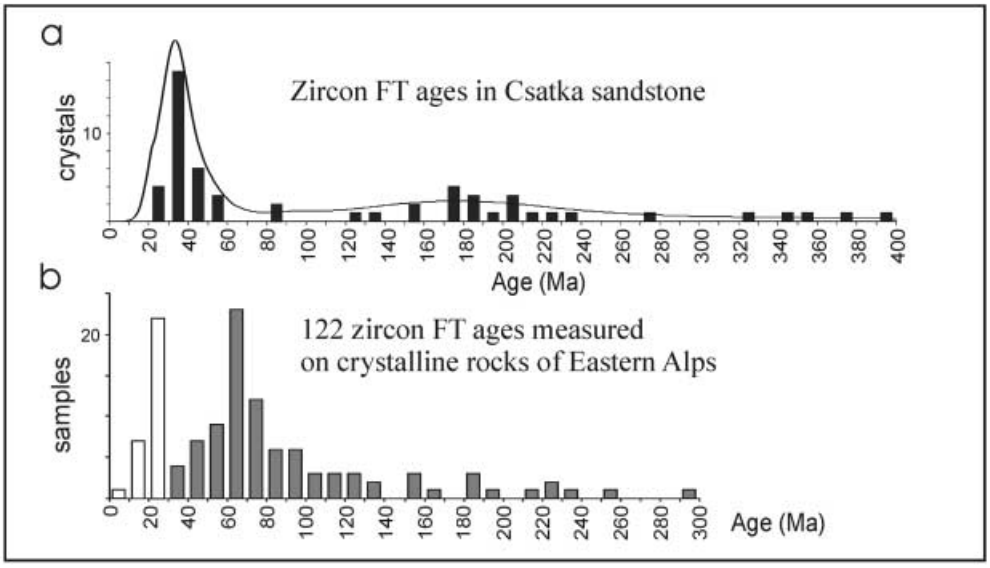

Fig. 11 **a** Age spectrum of single crystal zircon FT ages from a sandstone sample of the Csatka Formation; **b** compilation of zircon FT ages measured on Austroalpine rocks of the Eastern Alps from data of Flisch (1986), Fügenschuh et al. (1997), Elias (1998), Brix (unpublished), Dunkl (unpublished). *White bars* represent FT ages younger than the sedimentation of the Csatka Formation; thus they are insignificant in terms of the sediment provenance

line belt of the Eastern Alps; (2) the Austroalpine crystalline rocks were covered by molasse sediments; or (3) low-grade metamorphic rocks with Early Mesozoic zircon ages were covering the high-grade crystalline unit.

The fact that the surface geology of the Eastern Alps has changed since the Oligocene time has already been taken into account (Frisch et al. 1998). The composition of Bakony Molasse sediments proves that low-grade metamorphic rocks of the Eastern Alps (Greywacke zone + Gurktal Alps + Paleozoic of Graz) covered larger areas in the Late Oligocene than today. Thus, we prefer explanation (3), but the much broader sediment cover (2) in Oligo/Miocene time is also a plausible scenario.

Source areas, drainage system

Using the composition of amphiboles in tonalite (Hammarstrom and Zen 1986), the crystallization pressure ranges from 3.2–3.8 kbar, corresponding to an upper crustal environment of maximum 10–12 km. Based on these data, it follows that intensive erosion must have taken place in the source region of the igneous clasts between 30 Ma and the Late Oligocene,-Early Miocene.

The new geochronological data supported by the geochemistry make possible a more precise localization of the source areas. The following tectonic units of the western BM and the southern Eastern Alps were supplying sedimentary material to the Oligocene–Miocene Bakony Molasse (Fig. 12):

- Bakony Mountains: Permian sandstone, Eocene volcanic rocks;
- Periadriatic magmatic bodies: Oligocene tonalite, contact metamorphics;
- Drauzug: Permian sandstone; and
- Gurktal Alps, Paleozoic of Graz and Greywacke zone: low-grade schists, quartz, quartzites, rhyolite.

The Periadriatic lineament already formed a major eastward dewatering channel of the Alps in Eocene and Oligocene time (Kázmér and Kovács 1985). We consider that the Paleo-Drava river system transported the Alpine detritus to the southwestern Pannonian Basin. The Paleo-Drava, like the Paleo-Inn (Brügel et al. 2000), was localized along major faults formed during the Paleogene, and these rivers are the most persistent dewatering systems of the Eastern Alps.

Conclusions

1. The origin and transport of the Alpine-derived Oligo-Miocene sediment of the BM were primarily controlled by the activity of the Periadriatic lineament. Intermediate, calc-alkaline andesitic clasts form the majority of igneous clasts of the Csatka Formation. The age and geochemical characteristics of these samples indicate a close relationship to the Periadriatic magmatic belt. Traces of both Eocene and Oligocene volcanic phases are present.
2. The presence of volcanogenic material in the Late Oligocene molasse in the Pannonian Basin highlights the similarities of peri-Alpine molasse deposits of the same age.
3. Tonalite clasts derived from Periadriatic intrusions indicate possible exhumation of the subvolcanic level during the Late Oligocene. Zircon and apatite FT data prove that metasedimentary rocks with an Oligocene cooling age were also exhumed, transported and sedimented within the Csatka alluvial system.
4. Rhyolite clasts with Jurassic zircon FT age indicate source regions perhaps within the Eastern Alps.

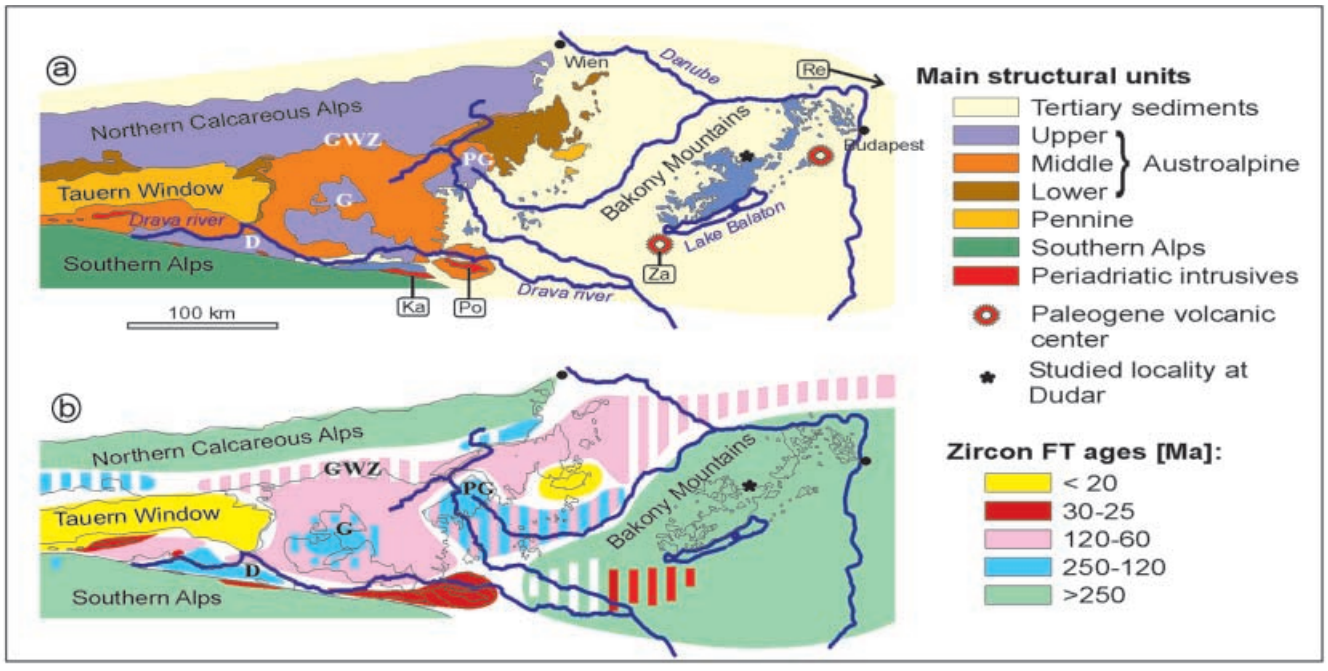

Fig. 12 **a** Geologic sketch map of Eastern Alps and western Pannonian realm (after Fuchs 1984). *PG* Paleozoic of Graz, *GWZ* Greywacke zone, *G* Gurktal Alps, *D* Drauzug. *Abbreviations* in frame indicate the localities of the samples of zircon morphological analyses: *Ka* Karavanks, *Po* Pohorje, *Za* Zala Basin, *Re* Recsk. **b** Areal distribution of zircon FT ages of the Eastern Alps and Bakony Mountains, compiled from data cited in Fig. 10. *White vertical stripes* indicate lack of data, where the characteristic zircon FT age is deduced from mica K/Ar ages; *coloured stripes* mark unknown boundaries or complex regions

5. Part of the sedimentary material was derived from the Bakony Mountains, but the Periadriatic magmatic bodies, the Drauzug, and the Upper Austroalpine units (Gurktal Alps, Greywacke zone) also made important detrital contributions to the Csatka Formation.
6. We propose that the ancestor of the recent Drava River was already in existence during the Oligocene, and dewatered the southern Eastern Alps along the Periadriatic fault in an eastward direction.

Acknowledgements The authors are grateful to K. Balogh (ATOMKI) for providing K/Ar data and thank O. Vaselli (University of Florence) for some of the whole rock analyses. K. Gál-Sólymos (Eötvös University) performed the microprobe analysis. The FT part of this study was financed by the German Science Foundation in the frame of the Collaborative Research Centre 275 (for I. Dunkl). This work was also supported by the Hungarian Scientific Research Fund (OTKA-A037/97 for S. Józsa). Thanks to M. Brix for the letter communicating his unpublished FT data. The final version of the manuscript benefited from the helpful comments of W. Frisch (Tübingen) and S.R. de la Rue (UMR). Constructive reviews by P.R.D. Mason and an unknown referee were much appreciated and improved both content and style. This is the No. 1 publication of the Lithosphere Research Group of the Department of Petrology and Geochemistry at Eötvös University, Budapest.

References

Árkai P, Lelkes-Felvári G (1987) Very low- and low-grade metamorphic terrains of Hungary. In: Flügel HV, Sassi FP, Grecula P (eds) IGCP Project No. 5 Regional Vol, Mineral Slovaca Monogr, pp 51–68

Bacon CR (1986) Magmatic inclusions in silicic and intermediate volcanic rocks. J Geophys Res 91:6091–6112

Baksa C (1975) The subvolcanic body of Recsk. Bull Hung Geol Soc 105:612–624

Baksa C, Csillag J, Földessy J (1974) Volcanic formations of the NE-Mátra mountains. Acta Geol Acad Sci Hung 18:387–400

Balázs E, Báldi T, Dudics E, Gidai L, Korpás L, Radócz G, Szentgyörgyi K, Zelenka T (1981) Structural-facial outline of Hungarian formations at the Eocene–Oligocene boundary. Bull Hung Geol Soc 111:145–156

Báldi T (1986) Mid-Tertiary stratigraphy and paleogeographic evolution of Hungary. Akadémiai Kiadó, Budapest

Báldi T, Báldi-Beke M (1985) The evolution of the Hungarian Paleogene Basin. Acta Geol Hung 28:5–28

Balogh K (1985) K/Ar dates of some Hungarian Late Eocene–Early Oligocene samples. Discuss Palaeont Fasc 31:49–51

Bellieni G, Peccerillo A, Poli A (1981) The Vedrette di Ries (Riesenferner) plutonic complex: petrological and geochemical data bearing on its genesis. Contrib Mineral Petrol 78:145–156

Bellieni G, Peccerillo A, Poli G, Fioretti A (1984) The genesis of Late Alpine plutonic bodies of Rensen and Monte Alto (Eastern Alps): inferences from major and trace element data. Neues Jahrb Mineral Abh 149:113–224

Blanckenburg FV, Davies JH (1995) Slab breakoff: a model for syncollisional magmatism and tectonics in the Alps. Tectonics 14:120–131

Brandon MT (1992) Decomposition of fission-track grain-age distributions. Am J Sci 292:535–564

Brügel A (1998) Provenances of alluvial conglomerates from the Eastalpine foreland: Oligo-Miocene denudation history and drainage evolution of the Eastern Alps. Tübinger Geowiss Arb, Reihe A 40:168

Brügel A, Dunkl I, Frisch W, Kuhlemann J, Balogh K (2000) The record of Periadriatic volcanism in the Eastern Alpine Molasse zone and its paleogeographic implications. Terra Nova 12:42–47

Chappell BW (1991) Trace element analysis of rocks by X-ray spectrometry. Adv X-ray Anal 34:263–276
D'Argenio B, Mindszenty A (1995) Bauxites and related paleokarst: tectonic and climatic event markers at regional unconformities. Eclog Geol Helv 88:453–499
Darida-Tichy M (1987) Paleogene andesite volcanism and associated rock alteration (Velence Hills, Hungary). Geol Carpathica 38:19–34
Downes H, Pantó G, Póka T, Mattey DP, Greenwood PB (1995) Calc-alkaline volcanics of the Inner Carpathian arc, Northern Hungary: new geochemical and oxygen isotopic results. Acta Vulcanol 7:29–41
Dunkl I (1990) Fission track dating of tuffaceous Eocene formations of the North Bakony Mountains (Transdanubia, Hungary). Acta Geol Hung 33:13–30
Dunkl I, Demény A (1997) Exhumation of the Rechnitz window at the border of Eastern Alps and Pannonian Basin during Neogene extension. Tectonophysics 272:197–211
Dunkl I, Nagymarosy A (1992) A new tie-point candidate for the Paleogene timescale calibration: fission track dating of tuff layers of Lower Oligocene Tard Clay (Hungary). Neues Jahrb Geol Paläont Abh 186:345–364
Dunkl I, Frisch W, Kuhlemann J, Brügel A (1996) "Combined-pebble-dating": a new tool for provenance analysis and for estimating Alpine denudation. Int Workshop on Fission-Track Dating, Gent, Abstr Vol, p 32
Dunkl I, Frisch W, Kuhlemann J (1999) Fission track record of the thermal evolution of the Eastern Alps – review of the main zircon age clusters and the significance of the 160 Ma event. Abstr 4th Workshop on Alpine Geological Studies, Tübingen. Tübinger Geowiss Arb, Reihe A 52:77–78
Eichelberger JC (1978) Andesitic volcanism and crustal evolution. Nature 275:21–27
Elias J (1998) The thermal history of the Ötztal–Stubai complex (Tyrol, Austria/Italy) in the light of the lateral extrusion model. Tübinger Geowiss Arb, Reihe A 42:172
Faninger E (1976) Karavanski tonalit. Geol Razprave in Porozila 19:153–210
Flisch M (1986) Die Hebungsgeschichte der oberostalpinen Silvretta–Decke seit der mittleren Kreide. Bull Ver Schweiz Petrol–Geol Ing 53(123): 23–49
Frank W, Kralik M, Scharbert S, Thöni M (1987) Geochronological data from the Eastern Alps. In: Flügel HW, Faupl P (eds) Geodynamics of the Eastern Alps. Deuticke, Vienna, pp 272–281
Franzini M, Leoni L, Saitta M (1975) Revisione di una metodologia analitica per fluorescenza X basata sulla correzione completa degli effetti di matrice. Rend Soc Ital Mineral Petrol 31:365–378
Frisch W, Kuhlemann J, Dunkl I, Brügel A (1998) Palinspastic reconstruction and topographic evolution of the Eastern Alps during late Tertiary extrusion. Tectonophysics 297:1–15
Fuchs W (1984) Grosstectonische Neuorientierung in der Ostalpen und Westkarpaten unter Einbeziehung plattentektonischer Gesichtepunkte. Jahrb Geol Bundesans Austria 127:571–631
Fügenschuh B, Seward D, Mancktelow N (1997) Exhumation in a convergent orogen: the western Tauern window. Terra Nova 9:213–217
Gelati R, Napolitano A, Valdisturlo A (1988) La "Gonfolite Lombarda": stratigrafia e significato nell'evoluzione del margine Sudalpino. Riv Ital Paleont Strat 94:285–332
Gieger M, Hurford AJ (1989) Tertiary intrusives of the Central Alps: their Tertiary uplift, erosion, redeposition and burial in the South Alpine foreland. Eclog Geol Helv 82:857–866
Gill J (1981) Orogenic andesites and plate tectonics. Springer, Berlin Heidelberg New York
Haas J, Kovács S, Krystyn L, Lein R (1995) Significance of Late Permian–Triassic facies zones in terrane reconstruction in the Alpine–North Pannonian domain. Tectonophysics 242:19–40
Hammarstrom JM, Zen E (1986) Aluminium in hornblende: an empirical igneous geobarometer. Am Mineral 71:1297–1313
Harangi S, Szabó C, Józsa S, Szoldán Z, Árva-Sós E, Balla M, Kubovics I (1996) Mesozoic igneous suites in Hungary: implications for genesis and tectonic setting in the northwestern part of Tethys. Int Geol Rev 38:336–360
Harrison TM, Armstrong RL, Naeser CW, Harokal JE (1979) Geochronology and thermal history of the Coast Plutonic Complex, near Prince Rupert, British Columbia. Can J Earth Sci 16:400–410
Hejl E (1997) "Cold spots" during the Cenozoic evolution of the Eastern Alps. Tectonophysics 272:159–173
Horváth E, Tari G (1987) Middle Triassic volcanism in the Buda Mountains. Ann Univ Sci Sect Geol Budapest 27:3–16
Hurford AJ (1986) Cooling and uplift patterns in the Lepontine Alps South Central Switzerland and an age of vertical movement on the Insubric fault line. Contrib Mineral Petrol 93:413–427
Hurford AJ, Fitch FJ, Clarke A (1984) Resolution of the age structure of the detrital zircon populations of two Lower Cretaceous sandstones from the Weald of England by fission track dating. Geol Mag 121:269–277
Kázmér M, Kovács S (1985) Permian–Paleogene paleogeography along the eastern part of the Insubric–Periadriatic Lineament system: evidence for continental escape of the Bakony–Drauzug Unit. Acta Geol Hung 28:71–84
Korpás L (1981) Oligocene–Lower Miocene formations of the Transdanubian Central Mountains in Hungary. Ann Hung Geol Inst 64:1–140
Kralik M, Krumm H, Schramm M (1987) Low-grade and very low-grade metamorphism in the Northern Calcareous Alps and in the Greywacke zone: illite-crystallinity data and isotopic ages. In: Flügel HW, Faupl P (eds) Geodynamics of the Eastern Alps. Deuticke, Vienna, pp 164–178
Körössy L (1988) Hydrocarbon geology of the Zala basin in Hungary. Gen Geol Rev Budapest 23:3–162
Läufer A, Frisch W, Steinitz G, Loeschke J (1997) Exhumed fault-bounded Alpine blocks along the Periadriatic lineament: the Eder unit (Carnic Alps, Austria). Geol Rundsch 86:612–626
Leake BE, Wooley AR, Arps CES, Birch WD, Gilbert MC, Grice JD, Hawthorne FC, Kato A, Kisch HJ, Krivovichev VG, Linthout K, Laird J, Mandarino JA, Maresch WV, Nickel EH, Rock NMS, Schumacher JC, Smith DC, Stephenson NCN, Ungaretti L, Whittaker EJW, Youzhi G (1997) Nomenclature of amphiboles: report of the Subcommittee on Amphiboles of the IMA, Commission on New Minerals and Mineral Names. Am Mineral 82:1019–1037
Lelkes-Felvári G, Árkai P, Sassi FP, Balogh K (1996) Main features of the regional metamorphic events in Hungary: a review. Geol Carpathica 47:257–270
Leonardi P (1967) Le Dolomiti, vol 1. Consiglio Nazionale delle Richerce, Trento
Leterrier J, Maury RC, Thonon P, Girard D, Marchal M (1982) Clinopyroxene composition as a method of identification of the magmatic affinities of paleo-volcanic series. Earth Planet Sci Lett 59:139–154
Macera P, Ferrara G, Pescia A, Callegari E (1983) A geochemical study on the acid and basic rocks of the Adamello batholith. Mem Soc Geol Ital 26:223–259
Mair V, Stingl V, Krois P, Keim L (1996) Die Bedeutung andesitischer und dazitischer Gerölle im Unterinntal-Tertiär (Tirol, Österreich) und im Tertiär des Mte. Parei (Dolomiten, Italien). Neues Jahrb Geol Paläont Abh 199:369–394
Müller W, Mancktelow N, Meier M, Oberli F, Villa I (1996) Dating of deformation across the brittle–ductile transition: high spatial resolution Rb/Sr and $^{40}Ar/^{39}Ar$ data from the Periadriatic fault system (Alps). V.M. Goldschmidt Conference, J Conf 1, p 415
Myers JD, Johnston AD (1996) Phase equilibria constraints on models of subduction zone magmatism. Subduction: top to bottom. Geophys Monogr 96:229–249

Nagymarosy A, Takigami Y, Balogh K (1986) Stratigraphic position and the radiometric age of the Kiscellian stratotype. Bull Liaisan Inf Proj 6:29–32

Nisbet EG, Pearce JA (1977) Clinopyroxene composition in mafic lavas from different tectonic settings. Contrib Mineral Petrol 63:149–160

Norrish K, Hutton JT (1969) An accurate X-ray spectrographic method for the analysis of a wide range of geological samples. Geochim Cosmochim Acta 33:431–453

Oberhauser R (1980) Der geologische Aufbau Österreichs. Springer, Vienna

Pearce JA (1982) Trace element characteristics of lavas from destructive plate boundaries. In: Thorpe RS (ed) Andesites: orogenic andesites and related rocks. Wiley, Chichester, pp 525–548

Pupin JP (1980) Zircon and granite petrology. Contrib Mineral Petrol 73:207–220

Rahn M, Stern WB, Frey M (1995) The origin of the Taveyannaz sandstone: arguments from whole-rock and clinopyroxene composition. Schweiz Mineral Petrogr Mitt 75:213–224

Royden LH, Báldi T (1988) Early Cenozoic tectonics and paleogeography of the Pannonian and surrounding regions. In: Royden LH, Horváth F (eds) The Pannonian Basin. A study in basin evolution. AAPG Mem 45, pp 1–16

Ruffini R, Polino R, Callegari E, Hunziker JC, Pfeifer HR (1997) Volcanic clast-rich turbidites of the Taveyanne sandstones from the Thônes syncline (Savoie, France): records for Tertiary postcollisional volcanism. Schweiz Mineral Petrogr Mitt 77:161–174

Sachsenhofer RF, Dunkl I, Hasenhüttl C, Jelen B (1998) Miocene thermal history of the southwestern margin of the Styrian Basin: coalification and fission track data from the Pohorje/Kozjak area (Slovenia). Tectonophysics 297:17–29

Stingl V, Krois P (1991) Marine fan development in a Paleogene interior-alpine basin: the basal Häring beds (Tyrol, Austria). Neues Jahrb Geol Paläontol Monatsh 7:427–442

Székyné FV, Barabás A (1953) Upper Eocene volcanic activity in Hungary. Bull Hung Geol Soc 79:217–229

Tari G, Báldi T, Báldi-Beke M (1993) Paleogene retroarc flexural basin beneath the Neogene Pannonian Basin: a geodynamic model. Tectonophysics 226:433–455

Tsuchiyama A (1985) Dissolution kinetics of plagioclase in the melt of the system diopside–albite–anorthite, and origin of dusty plagioclase in andesites. Contrib Mineral Petrol 89:1–16

Vörös A, Galácz A (1998) Jurassic palaeogeography of the Transdanubian Central Range (Hungary). Riv Ital Paleont Strat 104:69–84

Wenk HR, Hsiao J, Flowers G, Weibel M, Ayranci B, Fejér Z (1977) A geochemical survey of granitic rocks in the Bergell Alps. Schweiz Mineral Petrogr Mitt 57:233–265